

# QCD aspects of leptoquark production at HERA

C. Friberg<sup>1</sup>, E. Norrbin<sup>2</sup> and T. Sjöstrand<sup>3</sup>

*Department of Theoretical Physics,  
Lund University, Lund, Sweden*

## Abstract

If a leptoquark is produced at HERA as a narrow resonance, various effects tend to broaden the measurable mass distribution considerably. These effects are discussed here, with special emphasis on initial- and final-state QCD radiation. A proper understanding is important to assess the significance of data and to devise strategies for better mass reconstruction.

---

<sup>1</sup>christer@thep.lu.se

<sup>2</sup>emanuel@thep.lu.se

<sup>3</sup>torbjorn@thep.lu.se

Recently, the H1 and ZEUS Collaborations at HERA have presented evidence for an excess of events at large  $Q^2$  and  $x$  [1, 2]. This could be nothing but a statistical fluke. Alternatively, it could be the first signal of the production of an  $s$ -channel resonance, a leptoquark (LQ). In order to test such a hypothesis, as further data accumulate, it is important to understand the production characteristics of an LQ at HERA. In particular, it should be noted that an expected narrow mass peak will be smeared by various physics and detector effects. In this letter we want to give a brief survey of the physics components that could contribute to this smearing, and estimate the magnitude of each of these effects. Previous studies of a similar kind have been performed with the LEGO generator [3], which is partly based on PYTHIA [4]. We also want to give some examples of how to improve the reconstruction of the LQ mass.

This is not a study on the physics implications of an LQ observation at HERA [5]. Therefore we do not discuss the origin of an LQ in terms of an underlying theory, be that compositeness, supersymmetry or anything else, but stay with a purely phenomenological description of LQ properties [6]. Even so, several options are possible, and we will restrict ourselves further. An LQ may have spin 0 or 1, with differences in the decay angular distribution, but of little importance for the considerations in this letter, so we stay with the spin 0 alternative. An LQ may have net fermion number 0 ( $q\bar{\ell}$  or  $\bar{q}\ell$ ) or  $\pm 2$  ( $q\ell$  or  $\bar{q}\bar{\ell}$ ). Given that HERA has been running with an  $e^+$  beam in recent years, the latter kind would be disfavoured by requiring a sea antiquark from the proton. It would have been favoured in the earlier HERA runs with  $e^-$ , however, where the valence quark distributions could have been accessed. The ratio in parton distributions between valence and sea at  $x \approx 0.5$  being larger than the recorded luminosity ratio  $e^+p/e^-p$ , the previous non-observation [7] favours LQ's with vanishing fermion number. A leptogluon scenario is not excluded, but is not favoured [8]. QCD consequences of a  $\bar{q}\bar{\ell}$  LQ or a leptogluon are briefly mentioned later.

Phenomenologically, the production cross section for a leptoquark in the process  $q + \ell^+ \rightarrow \text{LQ}$  can be written as [6]

$$\sigma = \frac{\pi\lambda^2}{4s}q(x, M_{\text{LQ}}^2) = k\frac{\pi^2\alpha_{\text{em}}}{s}q(x, M_{\text{LQ}}^2) . \quad (1)$$

Here  $\lambda$  gives the strength of the unknown Yukawa coupling; the alternative  $k$  parameter is normalized such that  $k = 1$  corresponds to electromagnetic strength of the coupling. To first approximation  $x = M_{\text{LQ}}^2/s$  — corrections to this will be a main theme of the letter — and  $q(x, M_{\text{LQ}}^2)$  the parton distribution at a scale given by the LQ mass.

The observed handful of candidate events per experiments, for an integrated luminosity of order  $15 \text{ pb}^{-1}$  and a detection efficiency around 50% (including a cut  $Q^2 > 15000 \text{ GeV}^2$ ), would suggest a production cross section of the order of 1 pb. For a  $ue^+$  LQ of around 200 GeV mass this corresponds to  $k \sim 0.01$ . The width of a scalar LQ,

$$\Gamma_{\text{LQ}} = \frac{\lambda^2}{16\pi}M_{\text{LQ}} = \frac{k\alpha_{\text{em}}}{4}M_{\text{LQ}} , \quad (2)$$

then becomes only  $\Gamma_{\text{LQ}} \sim 4 \text{ MeV}$ . A  $de^+$  LQ would be somewhat broader, but in either case the width is negligibly small on an experimental scale. Unless the total width is enhanced significantly by decays to exotic channels, the LQ is long-lived enough that it will form an LQ-hadron, made up of the LQ and an antiquark or a diquark.

QCD radiation of gluons and QED radiation of photons in principle can occur in the initial state, off the LQ itself, and in the final state. Including all interference terms, a

complicated radiation pattern is then possible. The small width here offers a considerable simplification: interference terms and radiation off the LQ are suppressed for radiated energies above  $\Gamma_{\text{LQ}}$  [9, 10]. The region  $E \lesssim \Gamma_{\text{LQ}} \sim 10$  MeV giving a very small contribution to the total radiated energy, it is therefore sufficient to consider three main classes of corrections, (i) initial-state radiation, (ii) LQ-hadron formation, and (iii) final-state radiation. We will consider these effects one at a time, roughly in order of decreasing importance.

The main effect of final-state radiation is that the hadronic system of the LQ decay acquires a mass in excess of the naive quark one and that, as a consequence, the energy of the recoiling lepton is reduced. The jet mass phenomenology is not very different from experience in hadronic  $e^+e^-$  annihilation events. A standard parton-shower description [11] tuned to LEP data predicts an average quark jet mass of about 30 GeV at 200 GeV energy. Taking over the same formalism for the LQ decays then gives an average mass  $\langle M_q \rangle \approx 32$  GeV, Fig. 1, i.e. somewhat higher since the absence of a radiating final-state partner removes some phase-space competition. In a more detailed study one should include the explicit matrix-element information for the region of well-separated emission, which could introduce some modest dependence on the spin of the leptoquark.

In the rest frame of the LQ the lepton takes an energy

$$E_\ell = \frac{M_{\text{LQ}}}{2} \left( 1 - \frac{M_q^2}{M_{\text{LQ}}^2} \right). \quad (3)$$

The rest-frame lepton scattering angle  $\theta^*$  is only very little affected by the QCD radiation [12]. (Furthermore, for a spin 0 leptoquark, the inclusive decay distribution is isotropic in  $\cos \theta^*$  in any case.) Even though the standard DIS variables do not have the traditional meaning related to a spacelike boson propagator, they can be defined purely experimentally. The  $M_q$  term above then propagates to give

$$Q^2 = \frac{M_{\text{LQ}}^2}{2} (1 - \cos \theta^*) \left( 1 - \frac{M_q^2}{M_{\text{LQ}}^2} \right), \quad (4)$$

$$x_{\text{Bj}} = \frac{Q^2}{2Pq} = \frac{M_{\text{LQ}}^2}{s} \frac{Q^2}{Q^2 + M_q^2}. \quad (5)$$

Defining  $\tau$  to be the  $x$  value relevant for an LQ mass determination,

$$\tau \equiv \frac{\hat{s}}{s} = \frac{M_{\text{LQ}}^2}{s} = x_{\text{Bj}} \left( 1 + \frac{M_q^2}{Q^2} \right), \quad (6)$$

one finds that  $\tau > x_{\text{Bj}}$ . In particular note that the denominator of the  $M_q$  correction factor is  $Q^2$ , not  $M_{\text{LQ}}^2$ . This means that low- $Q^2$  data would not be expected to show any peak in  $x_{\text{Bj}}$ . A typical cut  $Q^2 > 15000$  GeV<sup>2</sup> reduces the  $\langle M_q \rangle$  from 32 GeV to 29 GeV (eq. (4)). The  $\langle M_q^2 \rangle \approx 1430$  GeV<sup>2</sup> then gives an average correction factor in eq. (6) of somewhat above 5%. If the experimentally reconstructed LQ mass is taken to be  $\sqrt{x_{\text{Bj}} s}$ , the original  $\delta$  function is smeared as shown in Fig. 2. Since  $Q^2 = x_{\text{Bj}} y s$  is an identity that follows from the definition of the respective variable, the alternative experimental measure  $\sqrt{Q^2/y}$  gives the same smearing.

Also photons may be radiated in the final state, both from the lepton and the quark. Owing to the smaller coupling, the amount of radiation is reduced compared with the QCD case above. Radiation almost collinear with the lepton occurs at a significant rate, but is

not resolved by the calorimetric definition of lepton energy and so is of little consequence. In our studies we choose not to resolve final-state photons below a 1 GeV invariant mass cut-off.

We next turn to initial-state radiation, i.e. radiation off the incoming quark and lepton lines. This reduces the longitudinal momentum fraction carried by the reacting quark/lepton, and builds up a  $p_\perp$  and a spacelike virtuality for it.

Photon radiation off the lepton line is dominated by the almost collinear one. In this limit, one has that  $\tau = x_q x_\ell$ , where the  $x_i$  are the respective momentum fractions. In the leading-log approximation, the positron-inside-positron distribution is roughly [13]

$$D_e^e(x_\ell, M_{LQ}^2) \approx \beta(1 - x_\ell)^{\beta-1} \quad \text{with} \quad \beta = \frac{\alpha_{em}}{\pi} \left( \ln \frac{M_{LQ}^2}{m_e^2} - 1 \right) \approx 0.0575. \quad (7)$$

The eq. (1) is then modified to

$$\sigma = k \frac{\pi^2 \alpha_{em}}{s} \iint dx_q dx_\ell q(x_q, M_{LQ}^2) D_e^e(x_\ell, M_{LQ}^2) \delta(x_q x_\ell - \tau). \quad (8)$$

One obtains  $\langle x_\ell \rangle \approx 0.99$  or  $\langle x_q \rangle \approx 1.01\tau$ . The steep fall-off of  $q(x_q, M_{LQ}^2)$  dampens the tail to large  $1 - x_\ell$ . Therefore typical experimental cuts on photon energy lost in the beam pipe do not make a big difference. The relation between the true and reconstructed masses is

$$\tau = x_{Bj} \frac{x_\ell^2}{1 - (1 - x_\ell)/y}, \quad (9)$$

so the mass shift may be in either direction, Fig. 2.

Radiation of photons and gluons in the initial state leads to a buildup of spacelike virtualities and transverse momenta for the incoming quark and lepton. The largest effects come on the quark side, Fig. 1, where  $\langle Q_q \rangle \approx 14.3$  GeV and  $\langle p_{\perp q} \rangle \approx 3.6$  GeV, while  $\langle Q_\ell \rangle \approx 0.85$  GeV and  $\langle p_{\perp \ell} \rangle \approx 0.15$  GeV for the incoming positron, using the spacelike parton-shower formalism of [14]. (Numbers vary a bit depending on choice of parton distribution parametrizations etc.) The spacelike virtualities can be seen as a kinematical consequence of the  $p_\perp$  kicks, so the  $Q_{q(\ell)}$  and  $p_{\perp q(\ell)}$  are strongly correlated. Note that  $\langle Q_q^2 \rangle \ll M_q^2$ : spacelike parton-shower evolution is constrained by the limited phase space and the steeply falling parton distributions at large  $x$ . That is, the probability that the daughter quark at  $x_i$  comes from the branching of a mother quark at  $x_{i-1} > x_i$  is related to the ratio  $q(x_{i-1})/q(x_i)$  of parton distributions, and the integral of  $q(x_{i-1})$  over  $x_{i-1} > x_i$  is small. At each branching one has  $p_{\perp i}^2 \approx (1 - z_i)Q_i^2$ , with  $z_i = x_i/x_{i-1}$ , so from the argument above it is clear why also  $\langle p_{\perp q}^2 \rangle \ll \langle Q_q^2 \rangle$ .

The consequences of nonzero virtualities and transverse momenta can again be traced through the standard DIS variables. Also including the previous effects, i.e.  $M_q \neq 0$  and  $x_\ell \neq 0$ , gives the relation

$$\tau = \frac{b - 2aQ_q^2 + \sqrt{b^2 - 4ax_\ell Q^2 (Q_q^2 - p_{\perp q}^2)}}{2sa},$$

where  $a = 1 - \frac{1-y}{x_\ell}$  (10)

and  $b = x_\ell Q^2 + M_q^2 + Q_q^2 - 2\bar{p}_{\perp q} \bar{k}'_{\perp}$ .

(A correction formula in terms of another set of variables is found in [3].) The spacelike virtuality and  $p_\perp$  kick may either increase or decrease the estimated LQ mass. In particular, there is an explicit dependence on the azimuthal angle between the  $p_{\perp q}$  of the

incoming quark ( $= p_{\perp\text{LQ}}$  in this approximation) and the  $k'_{\perp}$  of the outgoing lepton. The resulting spread in reconstructed LQ mass is shown in Fig. 2.

A  $p_{\perp q}$  contribution is also given by the primordial  $k_{\perp}$  of the parton-shower initiator inside the proton. This primordial  $k_{\perp}$  is some combination of Fermi motion and initial-state radiation below the soft cut-off of the simulation program. A typical scale for the former would be  $\langle k_{\perp}^2 \rangle \approx 0.25 \text{ GeV}^2$ , but even if this is increased to  $1 \text{ GeV}^2$  the net effects are quite negligible, since the  $k_{\perp}$  is added to the much larger  $p_{\perp}$  of the perturbative parton shower. Only in some future study of the LQ  $p_{\perp}$  distribution itself would the low- $p_{\perp\text{LQ}}$  tail be sensitive to the choice.

The effects of LQ-hadron formation are not large, since the LQ is so massive that its motion is not significantly affected by hadronization effects. Data on b and c quarks are consistent with a non-perturbative fragmentation where the LQ-hadron retains an average fraction

$$z \approx \frac{M_{\text{LQ}}}{M_{\text{LQ}} + 1 \text{ GeV}} \approx 0.995 \quad (11)$$

of the original LQ momentum, cf. [15]. The antiquark (diquark) contributes a typical fragmentation  $p_{\perp}$  to the net  $p_{\perp}$  of the LQ-hadron. The LQ has some Fermi motion inside the LQ-hadron, of the order of the antiquark constituent mass, that shifts the momentum of the decaying LQ. The net effects of all the hadronization contributions should be a more-or-less random momentum shift at or below the 1 GeV scale, i.e. negligible. A consequence of confinement is that the LQ mass cannot be defined unambiguously, so the detailed effects of hadronization have to be seen in the context of some specific scheme for relating the LQ-hadron mass to the LQ mass itself.

The hadronic system will show some effects of the LQ lifetime. If an LQ-hadron is formed, the hadrons produced from the proton remnant and the initial-state-radiation partons decouple completely from those produced in the decay of the LQ-hadron. This means, e.g., that the charged multiplicity is independent of the LQ decay angle, i.e. of  $Q^2$  (apart from some small trigger-bias effects). By contrast, if the LQ is too short-lived for LQ-hadron formation, the initial- and final-state partons are connected into a common colour string [16]. The string length and hence the multiplicity now depends on the angle between the proton remnant and the LQ hadronic decay products (just like in standard DIS processes, with  $W^2 \propto Q^2$  for fixed  $x_{\text{Bj}}$ ). If the initial- and final-state shower effects are neglected, the variation at small  $Q^2$  is significant, but is reduced to  $\sim 10\%$  in the  $Q^2 > 15000 \text{ GeV}^2$  region. When showers are included, however, these tend to dominate the particle production characteristics in a global sense. A memory remains in the soft (low-momentum) region, e.g. defined by  $|\mathbf{p}| < 1 \text{ GeV}$  in the longitudinal rest frame of the LQ. (The lab frame is unsuitable, since the LQ motion in this frame introduces large spurious effects.) Over the standard high- $Q^2$  range, and with full inclusion of parton showers, the variation in charged multiplicity is here over 20%. In the unlikely event that the LQ is very short-lived, coherence effects will also appear in the parton-shower stage, and so the multiplicity variation will spread to all  $|\mathbf{p}| \lesssim \Gamma_{\text{LQ}}$ . It is therefore possible to conclude from the hadronic final state whether an LQ-hadron is being formed or not, given enough statistics. This situation is quite similar to the one for the top quark [10].

All the physics aspects described above are included in the PYTHIA event generator [4].<sup>4</sup> The net distribution of reconstructed LQ masses is shown in Fig. 3, where all effects described above have been included. The bulk of the mass spread is given by the effects

---

<sup>4</sup>LQ-hadron formation is not part of the standard distribution. Note that `MSTJ(50)=0` and `MSTP(67)=0` should be set to switch off interference between the initial- and final-state radiation.

in eq. (10). After correction with this formula, the remaining mass spread is the result of the  $k_{\perp}$  kick and virtuality of the incoming lepton, the QED radiation off the outgoing lepton, and LQ-hadron formation.

A  $\bar{q}\bar{\ell}$  LQ would share most of the features described above. There is enhanced initial-state QCD radiation in those events where a branching chain  $q \rightarrow qg, g \rightarrow q\bar{q}$  occurs. However, most events start with a  $\bar{q}$  at the cut-off scale  $Q_0 \approx 1$  GeV, and here gluon radiation off the  $\bar{q}$  is suppressed by the steeply falling  $\bar{q}(x)$  distribution. That is, parton-shower histories that allow a  $\bar{q}$  to survive at large  $x$  and large  $Q^2$  are biased towards lower activity (a bit more than those of the  $q$ ), and so the  $\langle Q_{\bar{q}} \rangle \approx 12.4$  GeV rather than the 14.3 GeV of the  $q$ . For a leptogluon, an increased radiation in the final state follows directly from the higher colour charge,  $\langle M_g \rangle \approx 45$  GeV. In the initial state, there is again a suppression from the steeply falling gluon distribution. About half of the events contain a branching step  $q \rightarrow qg$ , and this branching is biased towards higher virtualities since the quark line below the branching scale radiates less than the gluon above. The net result is a fairly large mean,  $\langle Q_g \rangle \approx 31$  GeV. A leptogluon would hence give a higher hadronic multiplicity than an LQ.

So far we have concentrated exclusively on one method for LQ mass reconstruction, based on the measurement of the scattered positron ( $Q^2$ ,  $x_{Bj}$  and  $y$ ). Alternative methods are used by the H1 and ZEUS collaborations. However, they all share some common assumptions, such as massless partons and  $p_{\perp}$  balance between the scattered positron and the recoiling hadronic system, and therefore do not recover the bulk of the smearing effects noted above. The optimal way to reconstruct a narrow(er) mass peak clearly is detector-dependent, and so must be worked out by the experimental collaborations. We here want to give some very general comments, however.

With an ideal detector, and good separation between the LQ decay products and the hadrons from the proton beam remnant, the four-momentum of the LQ could be reconstructed to give the LQ mass directly. Such an approach suffers from the calorimetric smearing of hadronic momentum measurements. Since the parton-shower activity spreads out hadrons, there is also no clean separation of hadrons. Therefore, alternatively, one could start from the better-measured positron momentum and then add corrections according to eq. (10), to give a mass estimate  $m_{\text{recon}} = \sqrt{\tau s}$ . In practice, some of the required terms turn out to be rather difficult to reconstruct from the observable hadronic final state. The most feasible correction is for the final-state QCD radiation, which we have seen to be the largest individual source of smearing, and which also tends to give a systematic bias in a mass determination. Two alternative methods have been compared for reconstructing  $M_q$ . In the first, all particles with a (pseudo)rapidity below 1.7 (except the lepton) are used to calculate an invariant mass that is associated with  $M_q$ . The cut is selected to minimize the misidentification of particles between the LQ-hadron and the remnant system. In the second method, a jet clustering algorithm [4] is used to find jets with an  $E_{\perp} \geq 10$  GeV inside an  $R = \sqrt{(\Delta\eta)^2 + (\Delta\varphi)^2} < 1$  cone, and an invariant mass is calculated for the particles belonging to the jet or jets. The jet threshold is here selected so that initial-state radiation is less likely to give rise to a jet. The reconstructed  $M_q$  is then used in eq. (6) to give a corrected LQ mass estimate. The distributions in Fig. 4 show that either correction factor does result in a narrower mass peak (the width is reduced from 11.1 to 8.2 GeV) and one that contains less systematic bias towards underestimating the correct mass (the average is shifted from 195.3 to 200.6 GeV).

In summary, we have shown that several QCD effects are at play in the production and decay of a leptokuark. These effects are fairly well understood from our experience in other

areas of high-energy physics. It is therefore possible to describe in detail the production characteristics. This knowledge may be useful to obtain less biased and narrower mass peaks, and also to devise other tests that could help to distinguish between leptoquark production and ordinary DIS phenomena.

## References

- [1] H1 Collaboration, C. Adloff et al, DESY 97-024
- [2] ZEUS Collaboration, J. Breitweg et al, DESY 97-025
- [3] K. Rosenbauer, thesis RWTH Aachen, PITHA preprint 95/16,  
[http://www.physik.rwth-aachen.de/group/pitha/1995/pitha1995\\_16.html](http://www.physik.rwth-aachen.de/group/pitha/1995/pitha1995_16.html)
- [4] T. Sjöstrand, Comput. Phys. Commun. **82** (1994) 74
- [5] G. Altarelli, J. Ellis, G.F. Giudice, S. Lola and M.L. Mangano, CERN-TH/97-40;  
H. Dreiner and P. Morawitz, hep-ph/9703279;  
J. Kalinowski, R. Rückl, H. Spiesberger and P.M. Zerwas, DESY 97-038;  
V. Barger, K. Cheung, K. Hagiwara and D. Zeppenfeld, MADPH-97-991
- [6] W. Buchmüller, R. Rückl and D. Wyler, Phys. Lett. **B191** (1987) 442
- [7] ZEUS Collaboration, M. Derrick et al, Phys. Rev. Lett. **75** (1995) 1006;  
H1 Collaboration, S. Aid et al, Phys. Lett. **B379** (1996) 319
- [8] J. Bijnens, in ‘Proceedings of the HERA Workshop’, ed. R.D. Peccei (DESY, 1988),  
Vol. 2, p. 819
- [9] V.A. Khoze, L.H. Orr and W.J. Stirling, Nucl. Phys. **B378** (1992) 413;  
V.S. Fadin, V.A. Khoze and A.D. Martin, Phys. Lett. **B320** (1994) 141;  
T. Sjöstrand and V.A. Khoze, Z. Phys. **C62** (1994) 281
- [10] V.A. Khoze and T. Sjöstrand, Phys. Lett. **B328** (1994) 466
- [11] M. Bengtsson and T. Sjöstrand, Phys. Lett. **B185** (1987) 435; Nucl. Phys. **B289**  
(1987) 810
- [12] R. Kleiss, Phys. Lett. **B180** (1986) 400
- [13] R. Kleiss et al., in ‘Z physics at LEP 1’, eds. G. Altarelli, R. Kleiss and C. Verzegnassi,  
CERN 89-08 (Geneva, 1989), Vol. 3, p. 143
- [14] T. Sjöstrand, Phys. Lett. **157B** (1985) 321;  
M. Bengtsson, T. Sjöstrand and M. van Zijl, Z. Phys. **C32** (1986) 67
- [15] J.D. Bjorken, Phys. Rev. **D17** (1978) 171
- [16] B. Andersson, G. Gustafson, G. Ingelman and T. Sjöstrand, Phys. Rep. **97** (1983)  
31

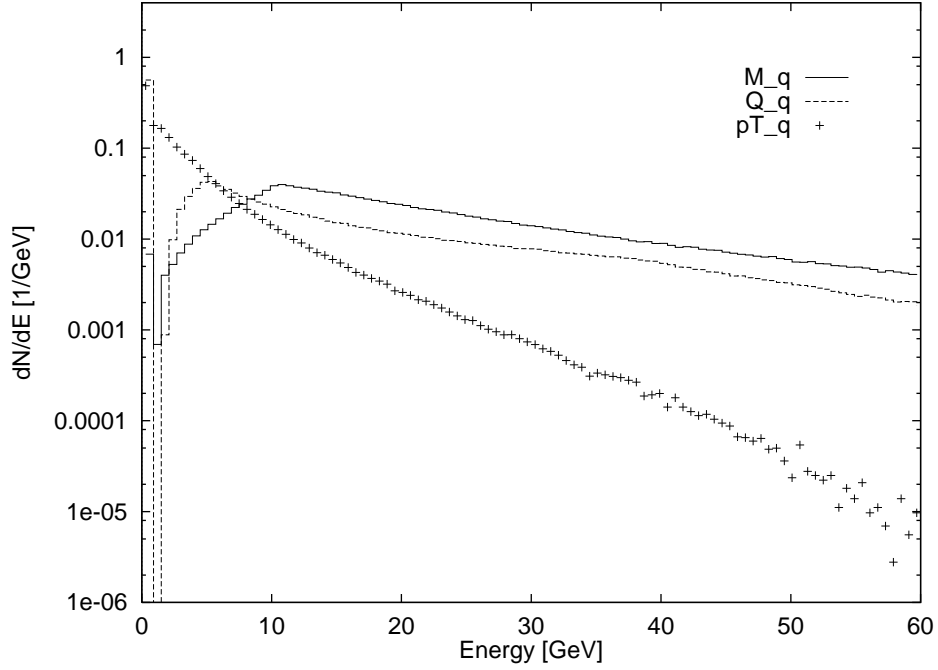


Figure 1: Distribution of  $M_q$  (full),  $Q_q$  (dashed) and  $p_{\perp q}$  (crosses).

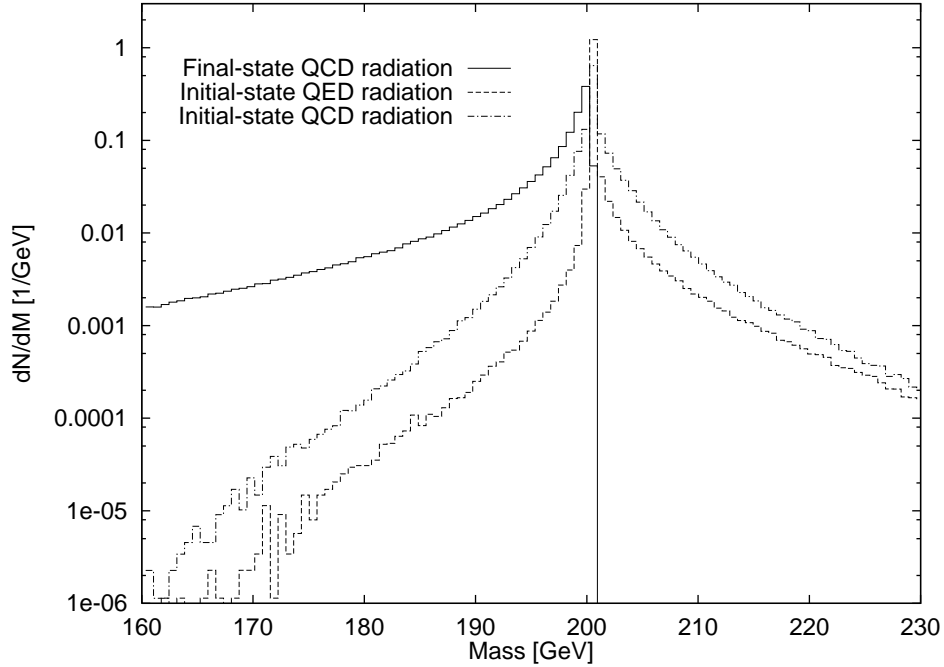


Figure 2: The reconstructed LQ mass distribution  $m_{\text{recon}} = \sqrt{x_{Bj}s}$  for an input mass of 200 GeV, with a simple cut  $Q^2 > 15000 \text{ GeV}^2$  on the leptoquark sample. Results are shown with only one component active at a time: final-state QCD radiation (full), initial-state QED radiation off the positron (dashed) and initial-state QCD radiation (dot-dashed).



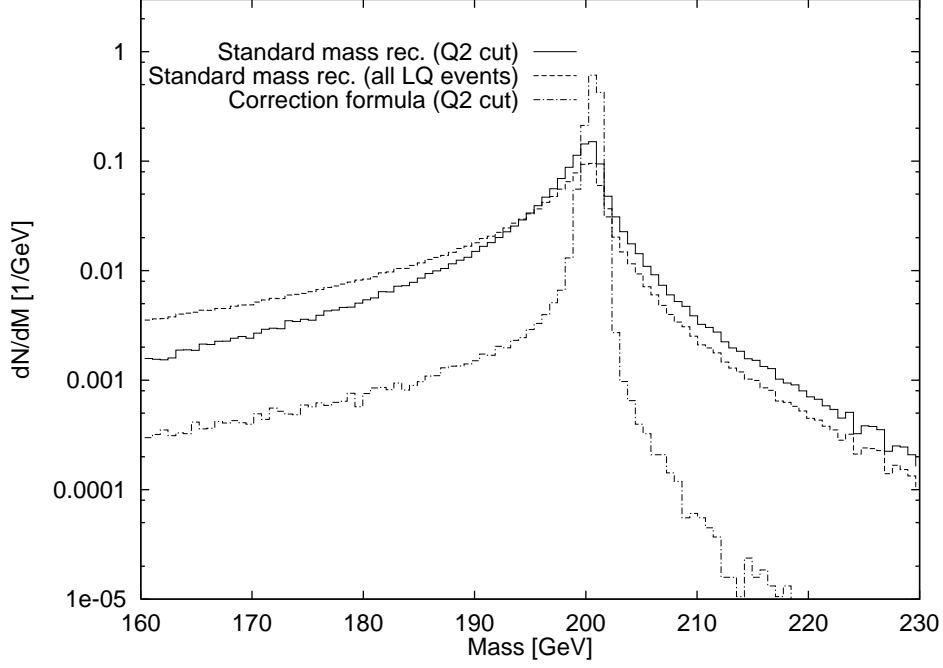


Figure 3: The reconstructed LQ mass distribution for an input mass of 200 GeV: all LQ events with  $m_{\text{recon}} = \sqrt{x_{\text{Bj}}s}$  (dashed),  $Q^2 > 15000 \text{ GeV}^2$  with  $m_{\text{recon}} = \sqrt{x_{\text{Bj}}s}$  (full) and  $Q^2 > 15000 \text{ GeV}^2$  with  $m_{\text{recon}} = \sqrt{\tau s}$ , eq. (10) (dot-dashed).

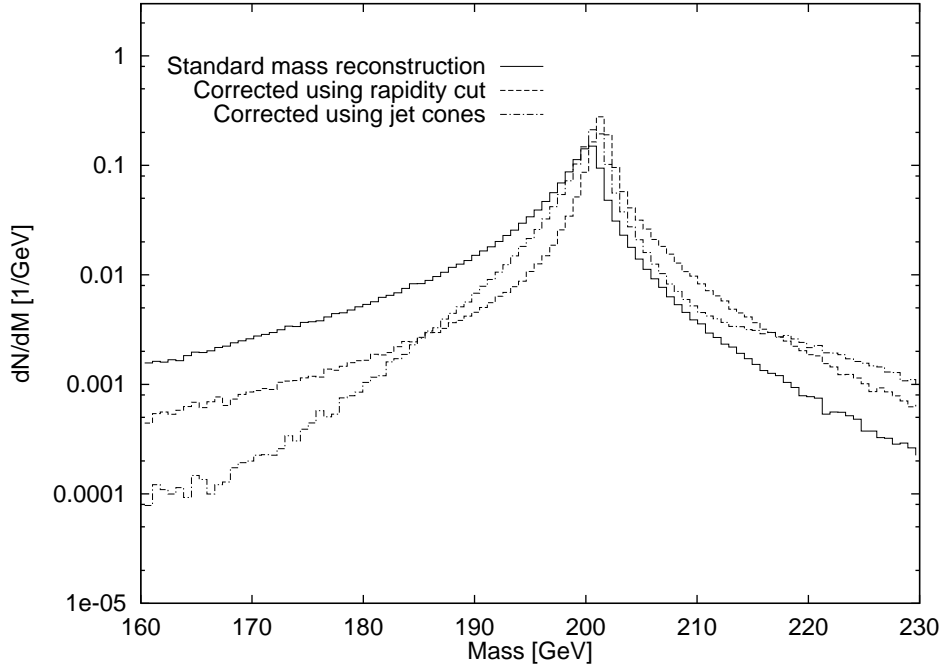


Figure 4: The reconstructed LQ mass distribution for an input mass of 200 GeV and with  $Q^2 > 15000 \text{ GeV}^2$ . Curves show mass based on  $x_{\text{Bj}}$  only (full), or corrected for  $M_q$  either with a pseudorapidity separation (dashed) or a jet-finding strategy (dot-dashed). For details see text.